NANO · MICRO small
www.small-journal.com

Polymer Brushes on Hexagonal Boron Nitride

Wenbo Sheng, Ihsan Amin, Christof Neumann, Renhao Dong, Tao Zhang,* Erik Wegener, Wei-Liang Chen, Paul Förster, Hai Quang Tran, Markus Löffler, Andreas Winter, Raul D. Rodriguez, Ehrenfried Zschech, Christopher K. Ober, Xinliang Feng, Andrey Turchanin, and Rainer Jordan**

Direct covalent functionalization of large-area single-layer hexagonal boron nitride (hBN) with various polymer brushes under mild conditions is presented. The photopolymerization of vinyl monomers results in the formation of thick and homogeneous (micropatterned, gradient) polymer brushes covalently bound to hBN. The brush layer mechanically and chemically stabilizes the material and allows facile handling as well as long-term use in water splitting hydrogen evolution reactions.

Progress in graphene research[1] has triggered tremendous interest in new types of 2D materials,[2] such as, e.g., hexagonal boron nitride (hBN).[3] Widely dubbed as the "white graphene," single-layer (SL) hBN nanosheet gained much attention due to their remarkable optical, mechanical, and electronic properties.[3] Many research efforts have been performed to functionalize hBN, either physical or covalent functionalization, to assure a broad range of applications.[4] Noncovalent functionalization of micrometer size hBN nanosheets has been reported.[5–7] Zhi et al.[5] demonstrated that mixing BN flakes with poly(methylmethacrylate) (PMMA) results in PMMA/BN composites with improved mechanical and thermal properties but at the expense of lower optical transparency as compared to pristine PMMA. Sainsbury et al.[7] reported the oxygen radical functionalization of micrometer-sized hBN nanosheets. The resulting surface hydroxyl groups could be further reacted with polymers. However, for many applications, a stable covalent functionalization is desired. Unlike graphene,[8] covalent functionalization of hBN sheets, especially with polymer brushes, has rarely been reported due to its extremely high chemically stability and resistance to oxidation even at temperatures above 800 °C.[9] Hence, it is particularly challenging to perform chemical reactions on the hBN lattice while preserving its intrinsic properties. Cui et al.[10] reported on the covalent functionalization of hydroxylated BN sheets with PMMA for enhanced nanofilllers. However, the use of very strong oxidation agents to obtain hydroxylated hBN for the functionalization is undesirable and a bottleneck for large-scale production. In general, the functionalization of hBN relies on multistep modification procedures with volatile and very aggressive chemicals. A more facile and safer chemical modification of hBN is therefore desirable. And to date, a covalent functionalization of large-area single-layer hBN with polymer brushes has not yet reported.

W. Sheng, Dr. I. Amin, Dr. T. Zhang, E. Wegener, P. Förster, Prof. R. Jordan
Chair of Macromolecular Chemistry
School of Science
Technische Universität Dresden
Mommsenstr. 4, 01069 Dresden, Germany
E-mail: ihsan.amin@inp-greifswald.de; tao.zhang@tu-dresden.de; rainer.jordan@tu-dresden.de

Dr. I. Amin
Junior Research Group Biosensing Surfaces
Leibniz Insitute for Plasma Science and Technology (INP)
Felix-Hausdorff-Str. 2, 17489 Greifswald, Germany

Dr. I. Amin, Prof. C. K. Ober
Department of Materials Science and Engineering
Cornell University
310 Bard Hall, Ithaca, NY 14853, USA

C. Neumann, Dr. A. Winter, Prof. A. Turchanin
Institute of Physical Chemistry
Friedrich Schiller University Jena
Center for Energy and Environmental Chemistry Jena (CEEC Jena)
Lessingstr. 10, 07743 Jena, Germany

DOI: 10.1002/smll.201805228

Dr. R. Dong, Dr. T. Zhang, Prof. X. Feng
Chair of Molecular Functional Materials
School of Science
Technische Universität Dresden
Mommsenstr. 4, 01069 Dresden, Germany

W.-L. Chen, H. Q. Tran
Robert Frederick Smith School of Chemical and Biomolecular Engineering
Cornell University
120 Olin Hall, Ithaca, NY 14853, USA

Dr. M. Löffler, Prof. E. Zschech
Dresden Center for Nanoanalysis
Center for Advancing Electronics Dresden (CfAED)
Technische Universität Dresden
Helmholtzstr. 18, 01187 Dresden, Germany

Prof. R. D. Rodriguez
Research School of Chemistry & Applied Biomedical Sciences
Tomsk Polytechnic University
30 Lenin Ave, 634050 Tomsk, Russia

Prof. E. Zschech
Department Head Microelectronic Materials and Nanoanalysis
Fraunhofer Institute for Ceramic Technologies and Systems
Maria Reiche Str. 2, 01099 Dresden, Germany

Here, we demonstrate the first example of direct grafting of polymer brushes on large-area SL hBN with a variety of vinyl monomers. The method is facile, catalyst and initiator free, and does not involve harsh reactants or conditions and results in homogeneous polymer brush coatings even on large-area SL hBN. Furthermore, graded or patterned polymer brushes on hBN are realizable. The functionalization of large-area SL-hBN with a variety of polymer brushes is realized by self-initiated photografting and photopolymerization (SIPGP),[11–13] analog to other 2D materials such as cross-linked self-assembled monolayers,[14] graphene oxide and graphene,[15,16] or graphene.[17] Herein, several vinyl monomers such as styrene (S), 4-vinylpyridine (4VP), methylmethacrylate (MMA), and *N,N*-dimethylaminoethyl methacrylate (DMAEMA) were successfully converted to polymer brushes, covalently bonded to SL-hBN. The chemical functionalization was monitored with X-ray photoelectron spectroscopy (XPS). The brush thicknesses were determined with atomic force microscopy (AFM) and ellipsometry. Contact angle measurements were performed to assess the wettability before and after the polymer grafting. The versatile SIPGP results in homogeneous, gradient and patterned brushes, and even consecutive SIPGP with different monomers is possible (e.g., poly[(styrene)-*g*-(4-vinylpyridine], PS-*g*-P4VP). The hBN–polymer brush composite was found to be mechanically robust as it could be detached from the supporting substrate and handled as freestanding polymer carpets. This new composite material may find numerous fields of applications such as sensing, actuation, energy storage, catalysis, optoelectronics, and others. As a first example of these applications, we further demonstrate the use of our hBN–polymer brush composites in water splitting hydrogen evolution reactions (HER). The surface-initiated polymerization of vinyl monomers on large-area SL-hBN nanosheets by SIPGP is outlined in **Figure 1**a.

Commercially available large-area (5 cm × 2.5 cm) chemical vapor deposition (CVD)-grown SL-hBN on copper foil[18] (Figure S1a, Supporting Information) was cut into pieces, 5 mm × 5 mm, and was transferred onto a silicon wafer (300 nm oxide layer) via PMMA-mediated transfer process.[19] Ellipsometry revealed a thickness of 0.5 nm ± 0.2 nm, which indicates the presence of an SL-hBN on the wafer substrate. The surface-initiated polymerization of vinyl monomers by SIPGP was performed by irradiation of SL-hBN sheets on

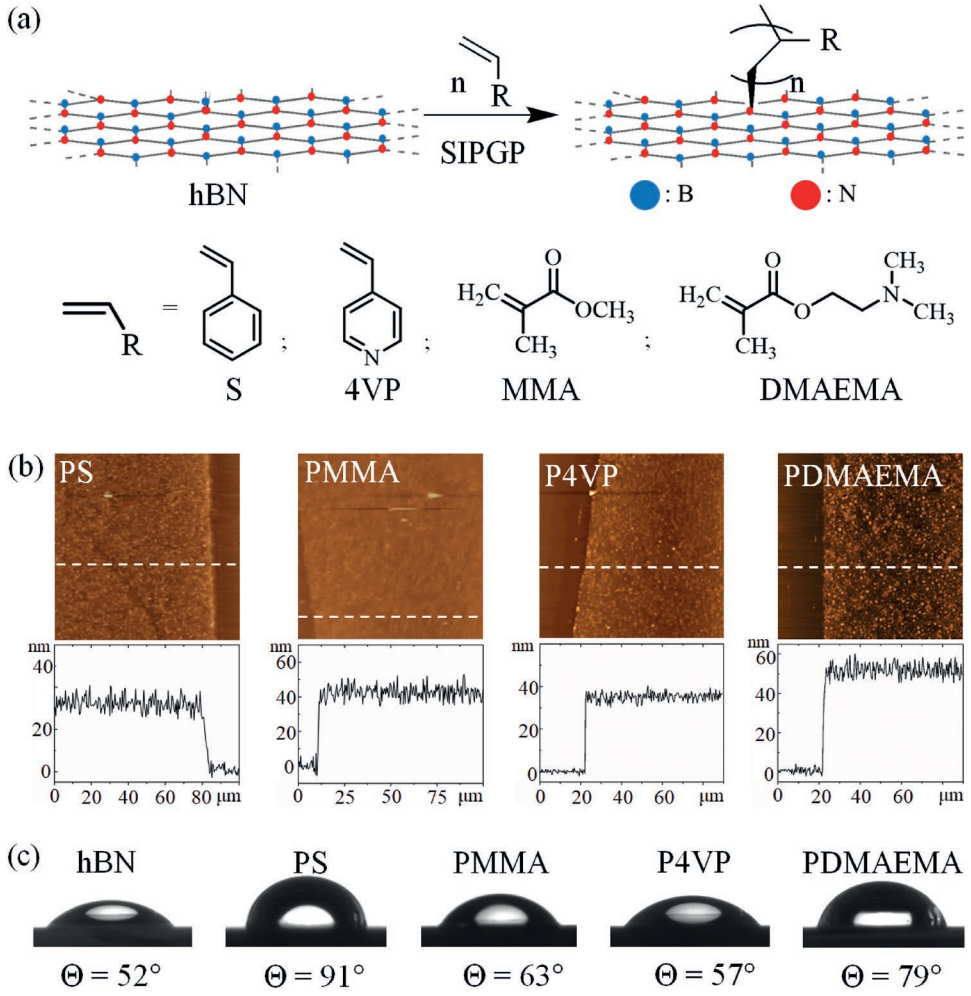

Figure 1. a) Schematic illustration of the direct modification of SL-hBN nanosheets by SIPGP of vinyl monomers under UV irradiation (monomers: S, 4VP, MMA, and DMAEMA). b) AFM height scans of samples and their corresponding height profiles. c) Contact angles of water on pristine hBN and on hBN after SIPGP of respected polymer brushes.

silicon supports immersed in degassed bulk monomer with UV light ($W \approx 5$ mW cm^{-2}, $\lambda_{max} = 365$ nm). As seen in Figure S1a (Supporting Information), only the areas with hBN showed significant changes in the optical appearance upon the SIPGP. The uniformity observed in the photographic images is a first indication of the formation of homogeneous polymer brushes over the entire hBN area. AFM measurements have revealed the following thicknesses for the brush layers: $d = 30 \pm 5$ nm for PS ($t_{SIPGP} = 12$ h), $d = 35 \pm 5$ nm for P4VP ($t_{SIPGP} = 8$ h), $d = 46 \pm 3$ nm for PMMA ($t_{SIPGP} = 6$ h), and $d = 50 \pm 8$ nm for PDMAEMA ($t_{SIPGP} = 4$ h) (Figure 1b). The surface roughness of as-grafted polymer brushes (Figure S1b, Supporting Information) is 3.08, 2.24, 4.02, and 3.91 nm for PS, P4VP, PMMA, and PDMAEMA, respectively, which is in the normal range and in good agreement with the literature.[12b] The obtained growth rates were $m = 2.2$ nm h^{-1} for PS and 13.4 nm h^{-1} for PDMAEMA, respectively (Figure S1b, Table S1, Supporting Information, for grafting density). In comparison, the growth rate of PS brushes on graphene is only about m = 1 nm h^{-1}[14] which indicates a higher grafting probability on hBN by the SIPGP mechanism involving surface radical formation on the 2D material. This difference might be accounted to the presence of defect sites/radicals in hBN and/or the nitrogen atoms in hBN. Previous studies showed the high grafting efficiency of SIPGP especially on amino-functionalized surfaces such as cross-linked SAMs of 4′-amino-1,1′-biphenyl-4-thiol on gold ($m = 7$ nm h^{-1})[11] and the same transferred to Si/SiO_2 substrates ($m = 35$ nm h^{-1}).[14] This high grafting efficiency is attributed to the low bond dissociation energy of the amino-hydrogen.[11] For the polymer grafting on graphene, local chemical defects appear to play a major role as the brush layer thickness is a direct function of the degree of hydrogenation of graphene.[17] Furthermore, the changes of the static water contact angle (Θ_S) from the pristine SL-hBN ($\Theta_S = 52°$) to the brush grafted hBN (hBN–PS: $\Theta_S = 91°$; –PMMA: $\Theta_S = 63°$; –P4VP: $\Theta_S = 57°$; –PDMAEMA: $\Theta_S = 79°$) further corroborate the successful formation of homogeneous polymer brush layers on the SL-hBN (Figure 1c).

To study the compositional quality of the polymer brushes and their grafting mechanisms, XPS analysis was performed on the transferred hBN sheets on SiO_2 substrates before and after grafting of polymer brushes (**Figure 2**). To this end, the thickness of the brushes was chosen <10 nm, in order to detect the N 1s and B 1s signals of the hBN. As shown in Figure 2a, for the native SL-hBN, the detected B 1s peak at 190.6 eV and the N 1s peak at 398.0 eV are in good agreement with previous reports.[18,20] The ratio of 1:1 for both elements confirms the high quality of the hBN films used for the polymer grafting. The small amount of carbon found in the sample fits to the signature of PMMA employed for the transfer of the hBN layer. For P4VP brushes (Figure 2b; Figure S2b, Supporting Information), the C 1s signal consists of C—C and C—N species as expected. Moreover, the pyridinic type of nitrogen at 399.5 eV found in the N 1s signal and the C:N ratio of 8 ± 1:1 fit to the chemical structure of the polymer confirming a successful grafting. A detailed analysis of the B 1s signal shows a shift of ≈0.5 eV of the boron peak toward higher binding energies indicated by the arrow in the figure. As this observation is found in a similar way for PS (Figure 2c) and PDMAEMA brushes (Figure S3, Supporting Information), we conclude the covalent binding of the polymer brushes via the boron atoms in the hBN film. This mechanism is different for PMMA brushes (Figure S4, Supporting Information), as the main component of the B 1s signal is not shifted (190.7 eV, green) and a significant amount of C—N bonds (399.8 eV, green) is found. Thus PMMA is most likely bound covalently to the N-sites of hBN, whereas the single species in the N 1s signal of PS at 398.4 eV do not indicate such binding. Due to the presence of other C—N species in P4VP and PDMAEMA only the grafting at boron sites can be detected. Similar to the formation of P4VP brushes, also the C 1s and N 1s spectra of PS, PDMAEMA, and PMMA confirm a successful grafting of the polymer brushes (Figure 2c; Figures S3 and S4, Supporting Information, respectively). Based on these XPS results, the proposed binding mechanism for all polymer brushes is depicted in Figure S5 (Supporting Information).

The grafting mechanism reported here corroborates with other reports on the functionalization of micrometer-sized hBN nanosheets[7,21] and BN nanotubes.[22,23] Wu et al.[22] demonstrated that the functionalization of boron nitride nanotubes (BNNTs) with NH_3 occurs on defect sites where the sidewall B atom is slightly pulled out of the surface and thus elongated. This structural deformation is attributed to the change of the local hybridization of the B atom from sp^2 to sp^3. A similar mechanism was reported by Sainsbury et al.,[7] who demonstrated the oxygen radical functionalization of micrometer-sized hBN nanosheets. The oxygen radical attacks the B atom and concomitant cleavage in the in-plane B—N bond occurs, leading to the formation of defects in the form of electron-deficient B atoms. The defects are further covalently functionalized with polymers (polyvinyl alcohol, PVA).

To further confirm the stability of the covalent binding of the polymer brushes to the hBN, the Soxhlet extraction experiments were performed for all polymer brush systems. As seen in Figure S6a (Supporting Information), for PS brushes grafted on SL-hBN, no significant changes observed after 80 cycles and the thickness are the same, while for physisorbed PS on SL-hBN, the layer was completely washed away even after 10 cycles. The same results are obtained for P4VP (Figure S6b, Supporting Information), PDMAEMA (Figure S6c, Supporting Information), and PMMA (Figure S6d, Supporting Information). These results clearly indicate that the stable covalent binding between the brushes and SL-hBN is formed during the SIPGP.

The chemical functionalization of SL-hBN, as described above, significantly broadens the applicability of hBN-based materials for device fabrication. However, an additional possibility to introduce defined heterogeneities into the polymer brush layers such as patterns, brush gradients, and multilayered brushes is desirable for advanced technologies.[24] Since the SIPGP is a photografting reaction, the preparation of micropatterned brushes is trivial and realizable with a photomask (Figure S7, Supporting Information). This direct patterning results in chemically heterogeneous surfaces containing the native hBN and the polymer brush. With SIPGP, patterned polymer brushes can also be generated from surfaces with areas of different probability of surface group abstraction.[14] This will result in polymer brushes covering the entire hBN surface but with different brush thicknesses.

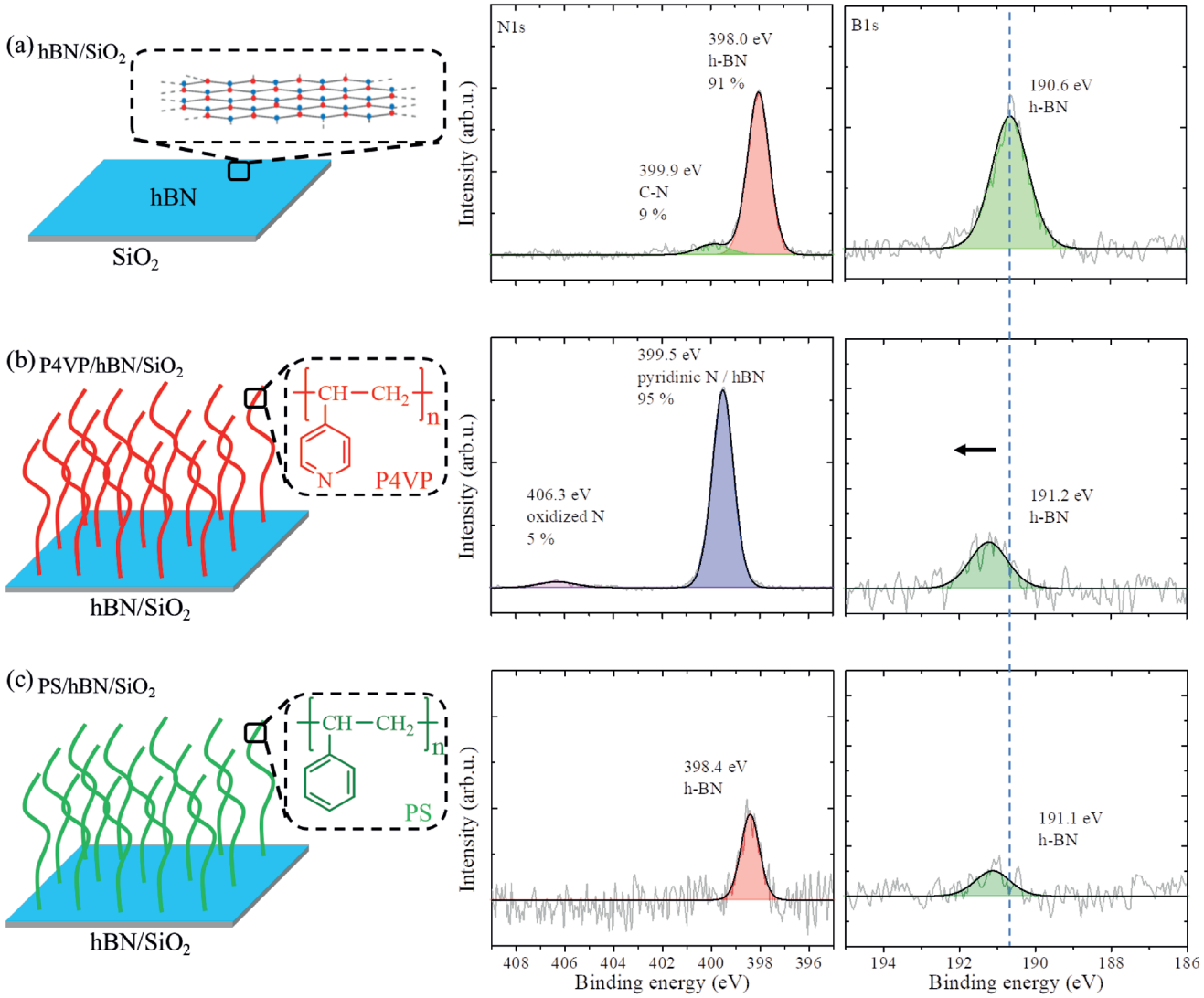

Figure 2. a–c) XPS analysis of polymer brushes grown on hBN transferred on SiO_2 substrates. In comparison to pristine hBN, the B 1s signal shifts toward higher binding energy after the polymer is grafted.

It has been shown that the carbon templating (CT) method is applicable to various substrates[25] including pristine single-layer graphene and results in polymer brush height gradients.[15] The CT uses focused-electron-beam lithography to deposit an amorphous carbonaceous layer as a function of the locally applied electron dose. A consecutive SIPGP amplifies the carbonaceous layer into a polymer brush at the irradiated locus and of a brush height that is a direct function of the electron dose applied. The CT allows the preparation of nano- and micropatterned brushes, brush gradients, and even 3D polymer structures.[13] Here, CT was used on SL-hBN to fabricate gradient (**Figure 3**a,b) and micropatterned polymer brush arrays (Figure 3c,d). A defined polymer brush gradient on SL-hBN was prepared by CT.[13] First, a carbon deposition was formed on the hBN by focused e-beam writing varying the local electron dose density linearly from 0 to 100 mC cm^{-2} (Figure 3a, upper image). The template was then amplified by SIPGP (1 h) using DMAEMA as the monomer. (Figure 3a, lower image). The AFM height image (Figure 3b) shows that the resulting brush layer thickness was found to be a direct function of the locally applied electron dose between 0 mC cm^{-2} (d = 20 nm, same as pristine hBN) and 40 mC cm^{-2} ($d \approx 140$ nm) and then stays constant. Such a relationship of the brush thickness and local electron dose is similar to earlier reports on other substrates and is explained by the local density of electron beam–deposited carbon on a respective substrate.[13] CT was also effective to prepare defined micropatterned brushes on SL-hBN over larger areas with an electron floodgun (an electron energy of 100 eV and a dose of 35 mC cm^{-2}) as the source and a stencil mask. The consecutive SIPGP step (styrene, t_{SIPGP} = 3 h) amplified the latent carbon pattern to micropatterned PS brushes on SL-hBN with a thickness of d = 30 nm (Figure 3c). A consecutive SIPGP step (4-vinylpyridine, 4VP, t_{SIPGP} = 3 h) results in micropatterned PS-*g*-P4VP brushes with a thickness of ≈300 nm (Figure 3d). In both cases, the patterning is created because of the preferred

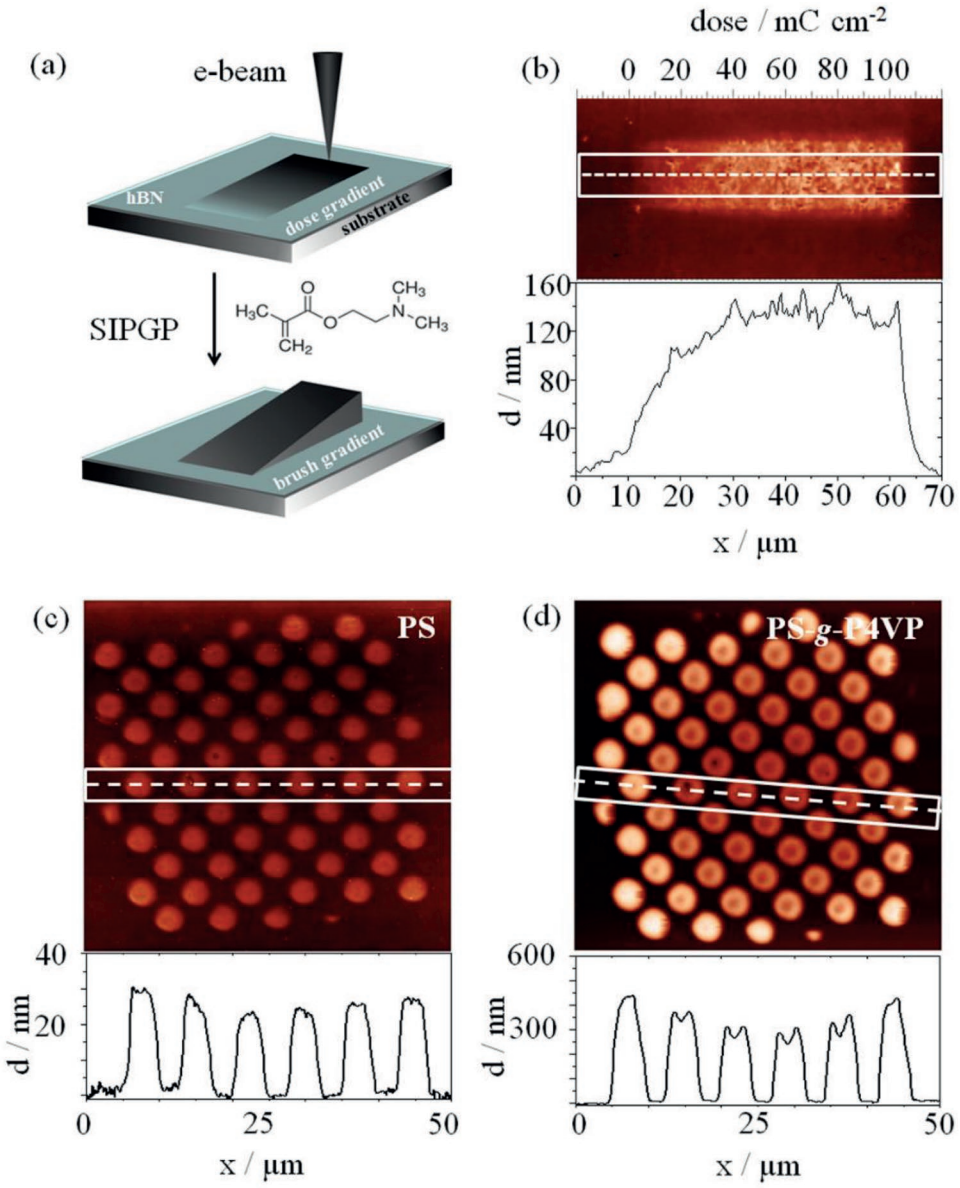

Figure 3. a) Schematic outline of the carbon templating (CT) procedure on SL-hBN. AFM height image of b) the PDMAEMA brush gradient and the corresponding height profile. c) AFM images of patterned PS brushes (30 nm) and d) PS-*g*-P4VP (≈300–400 nm) at the very same array of dots of the same sample after a consecutive SIPGP step.

grafting on the carbonaceous areas (or already grafted polymer) as compared to native hBN, but please note that a thinner brush is also formed on the native hBN ($d \approx 6$–7 nm for PS and $d = 13$ nm for P4VP).

One of the main difficulties of large-area 2D materials is their handling, especially the transfer of the atomically thin 2D materials from one to another substrate. Typically, a thin PMMA layer is spin-coated onto the 2D material for stabilization; the composite layer is removed from the substrate by etching; then transferred onto a desired substrate; and, finally, the PMMA layer is removed before further functionalization of the 2D materials. The polymer brushes grown on SL-hBN already present a chemical functionalization of the 2D materials and, moreover, the brushes provide mechanical stability of the material for further handling. This is demonstrated by the preparation of freestanding hBN–PS polymer carpets (Figure S8, Supporting Information). An SL-hBN was grafted with PS brushes (t_{SIPGP} = 12 h, d = 30 nm) by SIPGP then detached from the Si/SiO_2 substrate and then transferred onto a transmission electron microscopy (TEM) grid with 40 µm openings for imaging. As apparent from the optical microscopic images (Figure S8a, Supporting Information), the 30 nm thin polymer carpet could be transferred as a continuous sheet without cracks even by hand. Closer inspection reveals the appearance of characteristic wrinkles or buckles[14,26] because of the asymmetric carpet morphology and the strain imposed by the brush on the rigid 2D materials "substrate" (Figure S8b, Supporting Information).

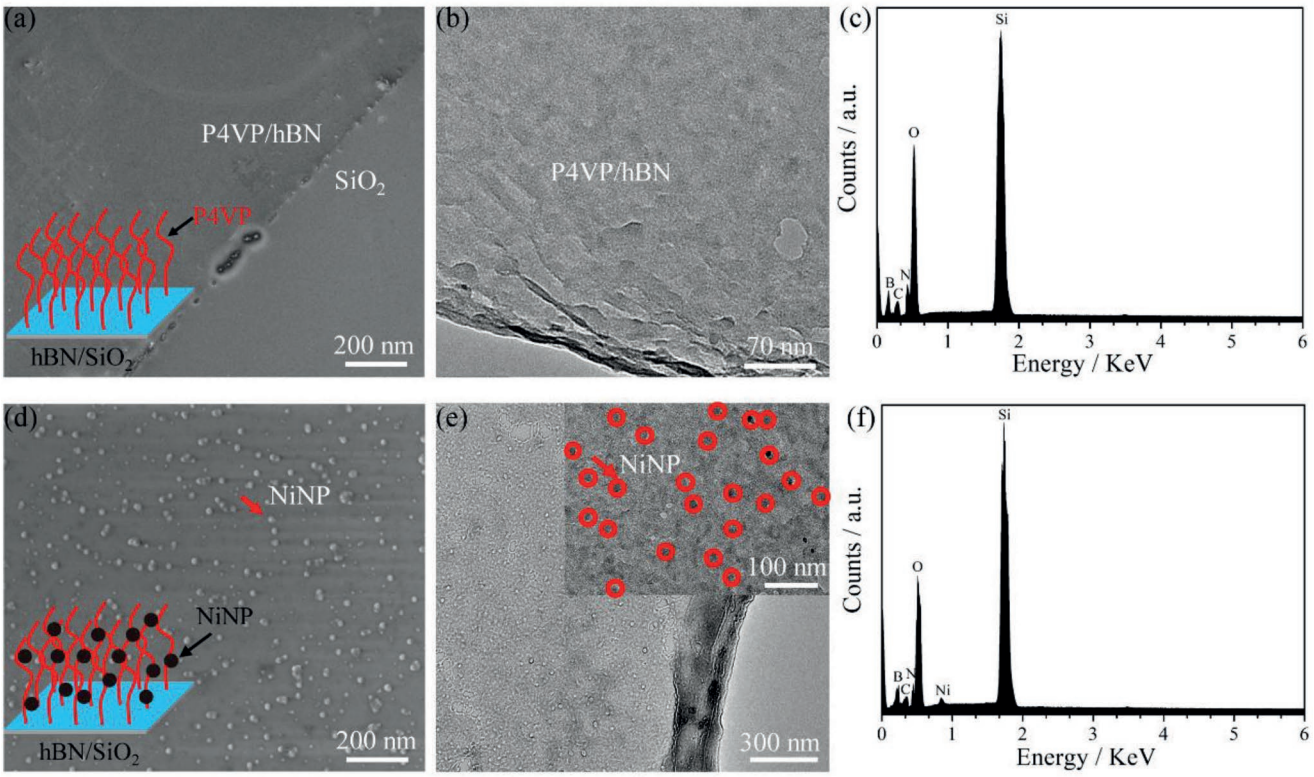

Figure 4. a) SEM and b) TEM images of P4VP-*g*-hBN. c) EDX spectra of panel (b). d) SEM and e) TEM images of NiNPs/P4VP-*g*-hBN. f) EDX spectra of panel (e).

The prepared hBN–polymer composites can be used for various applications.[27] As a first example, we demonstrate the application of P4VP-*g*-hBN for electrocatalytic water splitting to generate hydrogen, which is a promising clean and renewable energy carrier.[28] For this, the nickel nanoparticles (NiNPs, 0.1 M) were loaded into the P4VP brush similarly to a previously reported method.[29] As evidenced by scanning electron microscopy (SEM), TEM, and energy-dispersive X-ray spectroscopy (EDX) images in **Figure 4**, the NiNPs were successfully loaded within the P4VP brushes. NiNPs can be used as an alternative catalyst for HER, as they are much cheaper than other NP catalysts such as platinum or gold. Different hBN-based samples were prepared for the HER studies. NiNPs deposited directly on native SL-hBN (Ni-hBN) and NiNPs embedded in a P4VP brush grafted on hBN with a thickness of 10 (Ni-P10) or 100 nm (Ni-P100). The HER measurements were performed in 1 M KOH aqueous solution with a three-electrode configuration, using a Ag/AgCl electrode and a platinum wire as the reference electrode and counter electrode, respectively. The NiNP-loaded samples were transferred onto a Ti plate. As seen in **Figure 5**a, the prepared samples act as HER catalysts, with a current density reaching 10 mA cm^{-2} at an overpotential of 462 mV for Ni–hBN, 475 mV for Ni-P100, and 496 mV for Ni-P10. In Figure 5b, Tafel plots of the corresponding polarizations are displayed, providing further insights into HER reaction pathways.

These results highlight how the kinetics efficiency of water dissociation is facilitated by the catalysts. The Tafel slope recorded is 106 mV dec^{-1} for Ni–hBN, 118 mV dec^{-1} for Ni-P100, and 141 mV dec^{-1} for Ni-P10. These results suggest that the catalytic activities are in the following order: Ni–hBN > Ni-P100 > Ni-P10. However, during the measurements, the Ni–hBN and Ni-P10 layers detached from the counter electrodes and were found to be of insufficient stability, while the Ni-P100 remained stable throughout the HER studies. Further stability tests were performed with the Ni-P100 samples. After 1000 cyclic voltammetry (CV) cycles in 1 M KOH aqueous solution, the overpotential required for a current density of 10 mA cm^{-2} increased by only 10 mV (Figure 5c). A durability long-term HER process was performed at a current density of 10 mA cm^{-2}. As shown in Figure 5d, the thick Ni-P100 catalyst retained almost steady HER activity with an insignificant increase of 20 mV in the potential observed for hydrogen production over a period of 8 h. Additional HER with Ni-P100 performed in 0.5 M H_2SO_4 aqueous solution (inset, Figure 5a) revealed a lower performance for hydrogen evolution (cathodic current density reached 10 mA cm^{-2} at an overpotential of ≈621 mV) as compared to the catalyst activity in an alkaline solution. Because P4VP brushes swell in acidic solution while collapse in alkaline solution. When the P4VP brushes collapsed, the NiNPs are more compact within the polymer chains than that in swollen state, which will significantly enhance charge transfer in the composite film (NiNPs–P4VP-*g*-hBN). In comparison to similar systems (Table S2, Supporting Information),[30] a very good stability of the nickel-loaded P4VP-*g*-hBN catalyst allows the HER in alkaline as well as in acidic conditions.

In summary, we present the first example of direct functionalization of single-layer hBN with a broad variety of polymer brushes. The method is facile and does not require harsh

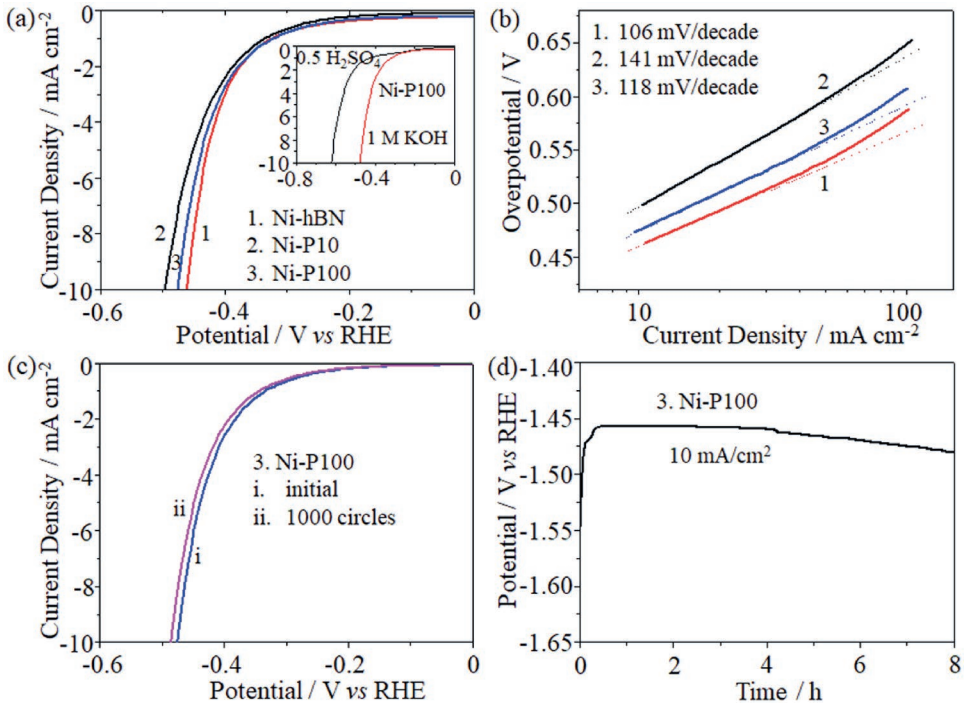

Figure 5. HER electrocatalytic activities of nickel nanoparticles deposited directly on hBN (Ni–hBN) or incorporated in the polymer brush of P4VP-*g*-hBN with 10 nm (Ni-P10) or 100 nm (Ni-P100) thickness (1 M $KOH_{aq.}$). a) Polarization curves. b) Tafel slopes of 1) Ni–hBN, 2) Ni-P10, and 3) Ni-P100. c) CV stability and d) 8 h operating durability of 3). Inset in panel (a) is a comparison of polarization curves of Ni-P100 samples in 1 M KOH and 0.5 M H_2SO_4.

reaction conditions or aggressive chemicals. The formed polymer layer effectively stabilizes hBN monolayers enabling its handling and implementation in devices. Furthermore, graded and micro-patterned polymer brush patterns can be prepared in this way. The implementation of hBN with grafted polymer brushes as a matrix material for catalytically active nickel nanoparticles demonstrates a significantly increase of the catalyst stability during hydrogen evolution reaction paving the way toward novel hydride 2D based materials for the electrocatalytic water splitting.

Experimental Section

Experimental methods and materials can be found in the Supporting Information.

Supporting Information

Supporting Information is available from the Wiley Online Library or from the author.

Acknowledgements

W.S. and R.J. acknowledge financial support from the Initiative and Networking Fund of the Helmholtz Association of German Research Centers through the International Helmholtz Research School for Nanoelectronic Networks, IHRS NANONET (VH-KO-606). I.A., W.S., and R.J. are thankful to the Center for advancing electronics Dresden (cfaed) for financial support. I.A. thanks the Graduate Academy TU Dresden and cfaed "Inspire Grant" for financial support during a research stay at Cornell University. I.A. thanks to Cornell NanoScale facility (CNF) for lab usage during the research stay at Ober's Group, Cornell University. W.-L.C., H.Q.T., and C.K.O. acknowledge support from CNF, a member of the National Nanotechnology Coordinated Infrastructure (NNCI), and National Science Foundation, NSF Grant ECCS-1542081, DMR-1306467, and DMR-1506542. Claudia Marschelke, IPF Dresden, is acknowledged for ellipsometry measurements of polymer brushes in different solvents. R.D.R. acknowledges the Tomsk Polytechnic University Competitiveness Enhancement Program. M.L. and E.Z. acknowledge the German Federal Ministry for Education and Research (BMBF) for support within the "MaKiZu" project. A.T., C.N., and A.W. acknowledge the Deutsche Forschungsgemeinschaft TRR-SFB 234 "CataLight" Projects B7 and Z2.

Conflict of Interest

The authors declare no conflict of interest.

Keywords

2D materials, hexagonal boron nitride, hydrogen evolution, patterning, polymer brushes

Received: December 9, 2018
Revised: March 2, 2019
Published online: April 1, 2019

[1] A. K. Geim, K. S. Novoselov, *Nat. Mater.* **2007**, *6*, 183.
[2] a) B. Dubertret, T. Heine, M. Terrones, *Acc. Chem. Res.* **2015**, *48*, 1; b) M. Xu, T. Liang, M. Shi, H. Chen, *Chem. Rev.* **2013**,

113, 3766; c) A. K. Geim, I. V. Grigorieva, *Nature* **2013**, *499*, 419; d) A. Turchanin, A. Gölzhäuser, *Adv. Mater.* **2016**, *28*, 6075; e) A. Turchanin, A. Golzhauser, *Prog. Surf. Sci.* **2012**, *87*, 108; f) H. Bian, X. Zhang, D. Huang, N. Zhang, *Chin. Chem. Let.* **2019**, *30*, 311.

[3] a) D. Golberg, Y. Bando, Y. Huang, T. Terao, M. Mitome, C. C. Tang, C. Y. Zhi, *ACS Nano* **2010**, *4*, 2979; b) D. Golberg, Y. Bando, Y. Huang, Z. Xu, X. L. Wei, L. Bourgeois, M. S. Wang, H. B. Zeng, J. Lin, C. Y. Zhi, *Isr. J. Chem.* **2010**, *50*, 405; c) Y. Lin, J. W. Connell, *Nanoscale* **2012**, *4*, 6908; d) A. Pakdel, Y. Bando, D. Golberg, *Chem. Soc. Rev.* **2014**, *43*, 934.

[4] Q. Weng, X. Wang, X. Wang, Y. Bando, D. Golberg, *Chem. Soc. Rev.* **2016**, *45*, 3989.

[5] a) C. Y. Zhi, Y. Bando, C. C. Tang, H. Kuwahara, D. Golberg, *Adv. Mater.* **2009**, *21*, 2889; b) X. B. Wang, A. Pakdel, J. Zhang, Q. H. Weng, T. Y. Zhai, C. Y. Zhi, D. Golberg, Y. Bando, *Nanoscale Res. Lett.* **2012**, *7*, 662.

[6] H. Wu, M. R. Kessler, *ACS Appl. Mater. Interfaces* **2015**, *7*, 5915.

[7] T. Sainsbury, A. Satti, P. May, Z. M. Wang, I. McGovern, Y. K. Gun'ko, J. Coleman, *J. Am. Chem. Soc.* **2012**, *134*, 18758.

[8] a) V. Georgakilas, M. Otyepka, A. B. Bourlinos, V. Chandra, N. Kim, K. C. Kemp, P. Hobza, R. Zboril, K. S. Kim, *Chem. Rev.* **2012**, *112*, 6156; b) A. Criado, M. Melchionna, S. Marchesan, M. Prato, *Angew. Chem., Int. Ed.* **2015**, *54*, 10734.

[9] a) Z. Liu, Y. J. Gong, W. Zhou, L. L. Ma, J. J. Yu, J. C. Idrobo, J. Jung, A. H. MacDonald, R. Vajtai, J. Lou, P. M. Ajayan, *Nat. Commun.* **2013**, *4*, 2541; b) L. H. Li, J. Cervenka, K. Watanabe, T. Taniguchi, Y. Chen, *ACS Nano* **2014**, *8*, 1457.

[10] Z. H. Cui, A. P. Martinez, D. H. Adamson, *Nanoscale* **2015**, *7*, 10193.

[11] M. Steenackers, A. Kuller, S. Stoycheva, M. Grunze, R. Jordan, *Langmuir* **2009**, *25*, 2225.

[12] a) A. N. Wright, *Nature* **1967**, *215*, 953; b) H. L. Wang, H. R. Brown, *Macromol. Rapid Commun.* **2004**, *25*, 1095; c) D. Hafner, L. Ziegler, M. Ichwan, T. Zhang, M. Schneider, M. Schiffmann, C. Thomas, K. Hinrichs, R. Jordan, I. Amin, *Adv. Mater.* **2016**, *28*, 1489; d) T. B. Stachowiak, F. Svec, J. M. J. Frachet, *Chem. Mater.* **2006**, *18*, 5950.

[13] M. Steenackers, R. Jordan, A. Küller, M. Grunze, *Adv. Mater.* **2009**, *21*, 2921.

[14] a) I. Amin, M. Steenackers, N. Zhang, A. Beyer, X. H. Zhang, T. Pirzer, T. Hugel, R. Jordan, A. Golzhauser, *Small* **2010**, *6*, 1623; b) I. Amin, M. Steenackers, N. Zhang, R. Schubel, A. Beyer, A. Golzhauser, R. Jordan, *Small* **2011**, *7*, 683.

[15] M. Steenackers, A. M. Gigler, N. Zhang, F. Deubel, M. Seifert, L. H. Hess, C. H. Y. X. Lim, K. P. Loh, J. A. Garrido, R. Jordan, M. Stutzmann, I. D. Sharp, *J. Am. Chem. Soc.* **2011**, *133*, 10490.

[16] T. Zhang, R. D. Rodriguez, I. Amin, J. Gasiorowski, M. Rahaman, W. Sheng, J. Kalbacova, E. Sheremet, D. R. T. Zahn, R. Jordan, *J. Mater. Chem. C* **2018**, *6*, 4919.

[17] M. Seifert, A. H. R. Koch, F. Deubel, T. Simmet, L. H. Hess, M. Stutzmann, R. Jordan, J. A. Garrido, I. D. Sharp, *Chem. Mater.* **2013**, *25*, 466.

[18] a) K. K. Kim, A. Hsu, X. T. Jia, S. M. Kim, Y. S. Shi, M. Hofmann, D. Nezich, J. F. Rodriguez-Nieva, M. Dresselhaus, T. Palacios, J. Kong, *Nano Lett.* **2012**, *12*, 161; b) K. K. Kim, A. Hsu, X. T. Jia, S. M. Kim, Y. M. Shi, M. Dresselhaus, T. Palacios, J. Kong, *ACS Nano* **2012**, *6*, 8583.

[19] A. Turchanin, A. Beyer, C. T. Nottbohm, X. Zhang, R. Stosch, A. Sologubenko, J. Mayer, P. Hinze, T. Weimann, A. Gölzhäuser, *Adv. Mater.* **2009**, *21*, 1233.

[20] a) Y. M. Shi, C. Hamsen, X. T. Jia, K. K. Kim, A. Reina, M. Hofmann, A. L. Hsu, K. Zhang, H. N. Li, Z. Y. Juang, M. S. Dresselhaus, L. J. Li, J. Kong, *Nano Lett.* **2010**, *10*, 4134; b) L. Song, L. J. Ci, H. Lu, P. B. Sorokin, C. H. Jin, J. Ni, A. G. Kvashnin, D. G. Kvashnin, J. Lou, B. I. Yakobson, P. M. Ajayan, *Nano Lett.* **2010**, *10*, 3209.

[21] a) Y. Lin, T. V. Williams, W. Cao, H. E. Elsayed-Ali, J. W. Connell, *J. Phys. Chem. C* **2010**, *114*, 17434; b) Y. Lin, T. V. Williams, J. W. Connell, *J. Phys. Chem. Lett.* **2010**, *1*, 277.

[22] X. J. Wu, W. An, X. C. Zeng, *J. Am. Chem. Soc.* **2006**, *128*, 12001.

[23] a) S. Y. Xie, W. Wang, K. A. S. Fernando, X. Wang, Y. Lin, Y. P. Sun, *Chem. Commun.* **2005**, 3670; b) C. Y. Zhi, Y. Bando, C. C. Tang, H. Kuwahara, D. Golberg, *J. Phys. Chem. C* **2007**, *111*, 1230; c) T. Ikuno, T. Sainsbury, D. Okawa, J. M. J. Fréchet, A. Zettl, *Solid State Commun.* **2007**, *142*, 643.

[24] a) T. Chen, I. Amin, R. Jordan, *Chem. Soc. Rev.* **2012**, *41*, 3280; b) B. P. Fors, J. E. Poelma, M. S. Menyo, M. J. Robb, D. M. Spokoyny, J. W. Kramer, J. H. Waite, C. J. Hawker, *J. Am. Chem. Soc.* **2013**, *135*, 14106; c) C. W. Pester, B. Narupai, K. M. Mattson, D. P. Bothman, D. Klinger, K. W. Lee, E. H. Discekici, C. J. Hawker, *Adv. Mater.* **2016**, *28*, 9292; d) J. E. Poelma, B. P. Fors, G. F. Meyers, J. W. Kramer, C. J. Hawker, *Angew. Chem., Int. Ed.* **2013**, *52*, 6844.

[25] a) M. Steenackers, S. Q. Lud, M. Niedermeier, P. Bruno, D. M. Gruen, P. Feulner, M. Stutzmann, J. A. Garrido, R. Jordan, *J. Am. Chem. Soc.* **2007**, *129*, 15655; b) M. Steenackers, I. D. Sharp, K. Larsson, N. A. Hutter, M. Stutzmann, R. Jordan, *Chem. Mater.* **2010**, *22*, 272.

[26] a) M. E. Welch, C. K. Ober, *ACS Macro Lett.* **2013**, *2*, 241; b) C. Ohm, C. K. Ober, *RSC Adv.* **2013**, *3*, 18482; c) P. Xiao, J. Gu, J. He, S. Wang, J. Zhang, Y. Huang, S.-W. Kuo, T. Chen, *J. Mater. Chem. C* **2016**, *4*, 9750; d) P. Xiao, C. Wan, J. Gu, Z. Liu, Y. Men, Y. Huang, J. Zhang, L. Zhu, T. Chen, *Adv. Funct. Mater.* **2015**, *25*, 2428.

[27] a) M. A. C. Stuart, W. T. S. Huck, J. Genzer, M. Muller, C. Ober, M. Stamm, G. B. Sukhorukov, I. Szleifer, V. V. Tsukruk, M. Urban, F. Winnik, S. Zauscher, I. Luzinov, S. Minko, *Nat. Mater.* **2010**, *9*, 101; b) W.-L. Chen, R. Cordero, H. Tran, C. K. Ober, *Macromolecules* **2017**, *50*, 4089; c) M. Welch, A. Rastogi, C. Ober, *Soft Matter* **2011**, *7*, 297; d) M. E. Welch, C. K. Ober, *J. Polym. Sci., Part B: Polym. Phys.* **2013**, *51*, 1457; e) M. E. Welch, Y. Y. Xu, H. J. Chen, N. Smith, M. E. Tague, H. D. Abruna, B. Baird, C. K. Ober, *J. Photopolym. Sci. Technol.* **2012**, *25*, 53; f) M. Kim, S. Schmitt, J. Choi, J. Krutty, P. Gopalan, *Polymers* **2015**, *7*, 1346; g) J. O. Zoppe, N. C. Ataman, P. Mocny, J. Wang, J. Moraes, H.-A. Klok, *Chem. Rev.* **2017**, *117*, 1105.

[28] a) J. Zhang, T. Wang, P. Liu, S. Liu, R. Dong, X. Zhuang, M. Chen, X. Feng, *Energy Environ. Sci.* **2016**, *9*, 2789; b) R. H. Dong, M. Pfeffermann, H. W. Liang, Z. K. Zheng, X. Zhu, J. Zhang, X. L. Feng, *Angew. Chem., Int. Ed.* **2015**, *54*, 12058; c) J. Zhang, S. H. Liu, H. W. Liang, R. H. Dong, X. L. Feng, *Adv. Mater.* **2015**, *27*, 7426; d) H. Sahabudeen, H. Qi, B. A. Glatz, D. Tranca, R. Dong, Y. Hou, T. Zhang, C. Kuttner, T. Lehnert, G. Seifert, U. Kaiser, A. Fery, Z. Zheng, X. Feng, *Nat. Commun.* **2016**, *7*, 13461.

[29] a) S. Gupta, M. Agrawal, M. Conrad, N. A. Hutter, P. Olk, F. Simon, L. M. Eng, M. Stamm, R. Jordan, *Adv. Funct. Mater.* **2010**, *20*, 1756; b) J. Chen, P. Xiao, J. Gu, Y. Huang, J. Zhang, W. Wang, T. Chen, *RSC Adv.* **2014**, *4*, 44480.

[30] a) H. Wang, W. Chen, J. Zhang, C. Huang, L. Mao, *Int. J. Hydrogen Energy* **2015**, *40*, 340; b) M. Zhukovskyi, P. Tongying, H. Yashan, Y. Wang, M. Kuno, *ACS Catal.* **2015**, *5*, 6615.